

Analysis of cosmic ray spectra with the GARFIELD array

G. Andreetta¹, L. Domenichetti¹, E. Vient^{1,2}.

¹ *Dipartimento di Fisica e Astronomia, Università di Padova, Padova, Italy;* ² *University of Caen, France.*

INTRODUCTION

In January 2021, an experiment of the ISOLIGHT campaign has been performed using the GARFIELD array. Before the experiment beam time, a two-day acquisition has been run collecting background data, in particular coming from cosmic rays. Such measurements are important to understand how GARFIELD is sensitive to this kind of radiation. Indeed, such background radiation is always present - being able to characterize it may lead to cleaner spectra when analysing data from an experiment, such as the one run in January.

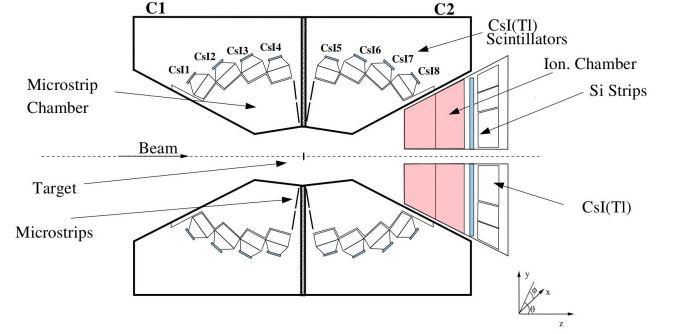


Fig. 1. Schematic picture of the GARFIELD+RCo section.

EXPERIMENTAL SETUP

The GARFIELD array [1] is a two-stage apparatus which exploits the ΔE - E identification technique. It has a cylindrical symmetry around the beam line and it is divided into two parts, the backward and the forward chambers. The target is placed in the middle between the two sections. The first stage consists of a drift chamber, filled with CF_4 gas, which provides the ΔE information. The E signal comes from a set of scintillating crystals, CsI(Tl) , placed in the outer part of the gas chamber and facing the interaction point. GARFIELD chambers are divided into 24 azimuth sectors ($\phi \approx 15^\circ$) and each sector contains 8 CsI(Tl) along the polar angle. A 45° gap on ϕ (sectors 24-1-2) in the backward chamber allows placing ancillary detectors. The readout of the scintillators is performed by photo-diodes placed on top of the CsI(Tl) themselves. The shape of such detectors is peculiar and custom-designed to guarantee a good angular coverage. The GARFIELD apparatus is often coupled to an ancillary detector, the Ring Counter. This detector is placed at low-forward angles to measure fragments ejected in that direction. It is a 3-stage detector, made up of an ionization chamber, followed by silicon strip detectors and CsI(Tl) scintillators. It was not used during the background data acquisition.

In the analysis run, only CsI were read - the drift chambers were not involved in the data acquisition. One of the main goals of such acquisitions was to check the detector-detector correlations in the Garfield array.

The signal from the scintillators was used as the trigger for the acquisition. To have a cleaner view of cosmic rays, no particular trigger settings have been tried online. If it may be of interest, particular correlations may be then analysed offline.

METHODS

The data collected were sorted using Garfield's predefined analysis macros, written exploiting a C++-ROOT environment. The output *.ROOT* file contains a TTree storing specific information on each event acquired. Among the variables available, the most important ones for the presented analysis are linked to scintillators: namely, the event multiplicity and a C++-object returning detailed information on the signals recorded by each CsI hit in the specific event. The most interesting attributes are:

- Ring (from 1 to 8) and Sector (1-24);
- Fast component of light signal;
- Slow component of light signal;
- A linear combination of fast and slow components;
- The time of arrival of the signal.

Through rings and sectors it is possible to reconstruct the position of the scintillator hit: an unambiguous identification of the CsI(Tl) n can be done using the following expression:

$$n = 10 \cdot n_{\text{sect}} + n_{\text{ring}} \quad (1)$$

where n_{sect} and n_{ring} are the identification numbers of Sector and Ring. Indeed, only 8 rings are present - so multiplying the sector by 10 avoids any possible overlap. Moreover, it is interesting to notice that this hashed variable has some holes - given that the ring ID ranges from 1 to 8, it is not possible to retrieve hashed IDs equal to x9 or x0, where x represents the sector number.

ANALYSIS

A constraint on the multiplicity was applied to select only single cosmic ray events. In particular, only multiplicity-2 events were considered. Therefore, an event is accepted if only two detectors were triggered. Then, a correlation matrix was built, plotting the number of events associated with the coincidence between different channels exploiting Eq. (1). The auto-coincidence was neglected and two noisy channels (hashed - 46 and 215) were identified and excluded from the correlation matrix.

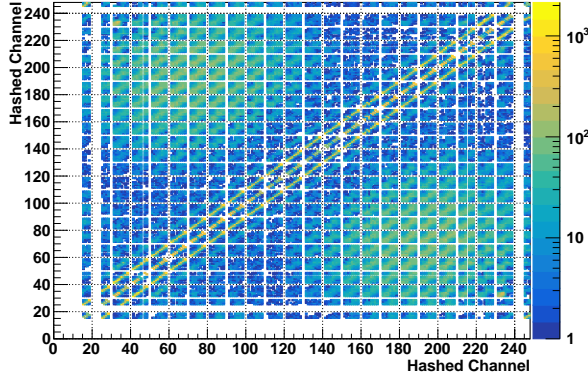


Fig. 2. Correlation matrix.

Fig. 2 shows a symmetric plot - this is due to the fact that both elements of each pair of hit detectors were displayed. The two main regions are the central one and the one in the top-left / bottom-right corners. The lines crossing the plot in the middle are linked to events in which detectors belonging to adjacent sectors were hit. Such events may be linked to Compton scattering events.

On the other hand, the regions in the corners are present only in coincidence with channels belonging to the upper and lower side of the detector. Such events are supposed to be due to cosmic rays impinging on the detector.

Moreover, an underlying structure can be seen throughout the whole figure: every little square has a peak in one of its diagonals. This is linked to a more favourable correlation between detectors belonging to the same ring. Geometrically, this is linked to detectors placed one on top of the other. Furthermore, this effect supports the attribution of this region to cosmic rays - indeed, the distribution of the angle of arrival of a cosmic ray has its maximum at $\theta = 0$, where θ is the angle with respect to the azimuth.

Such distribution may be interpreted more in detail concentrating on a single channel. Selecting only one "entrance" CsI(Tl), chosen on the top part of Garfield ($n \in [40; 100]$), it is possible to observe the distribution of events in which other scintillators triggered in coincidence with the selected one. In this way, it appears clearly the distribution of the cosmic rays hitting on the bottom part of Garfield ($n \in [140; 240]$).

In principle, this distribution should follow the

characteristic cosmic ray one, which is proportional to $\cos^2 \theta$. In practice, the nontrivial shape of Garfield's detector, the cylindrical symmetry, and the nonnull CsI(Tl) dimensions introduce a distortion in the distribution of the events. Nevertheless, we can observe in Fig. 3 that the maximum of the distribution is located along the vertical direction with respect to the position of the chosen entrance scintillator; then, the counts decrease moving from that position towards the adjacent detectors. To reproduce such a distribution with a reasonable accuracy, a simulation that takes into account all geometrical effects has to be considered.

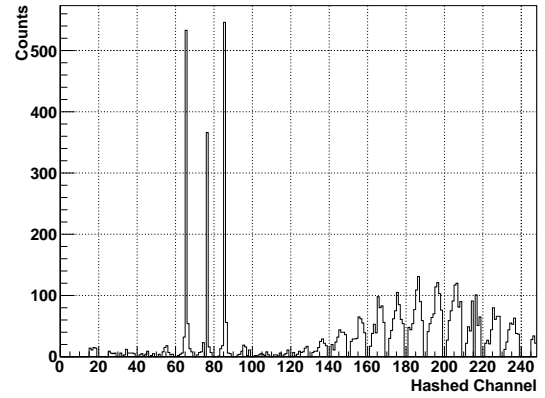


Fig. 3. Events distribution. Sector 7, Ring 5.

Finally, the last part of the analysis consisted in the study of the energy spectra released in each detector by different kinds of radiation. To exclude Compton-like events, only the regions in the corners were considered. Due to lack of time, a proper calibration of all detectors was unfeasible. Nonetheless, it is possible to notice that, focusing on a single scintillator and assuming a linear response of the detector, the whole procedure can be skipped. In figure 4 the energy spectrum obtained selecting sector 7 and ring 5 is shown.

The energy distribution is supposed to be following a Landau distribution. However, side effects have to be considered. First, the number of counts is not high enough - a calibration of the whole array would truly help statistics. Moreover, the highly irregular geometry of the scintillator itself affects the energy resolution - cosmic rays are in the Minimum Ionizing Particle regime of Bethe's formula, so their energy loss in the detector depends on the length of their path inside the CsI(Tl) scintillator. Therefore, the energy distribution does not appear as clear as expected, but taking into account all effects, the distribution seen in figure 4 is justified.

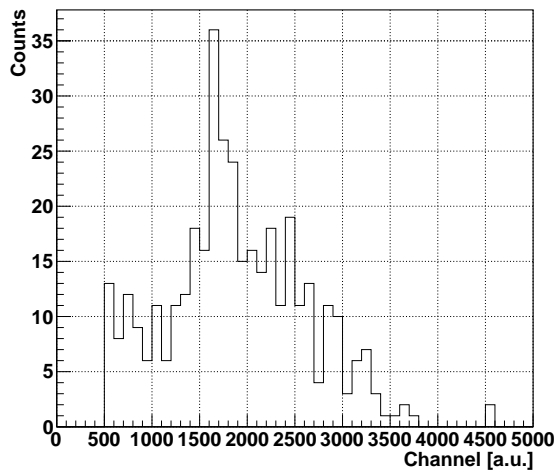


Fig. 4. Energy distribution. Sector 7, Ring 5.

CONCLUSION AND REFERENCES

The GARFIELD array is a multipurpose array which, in this experience, has been characterized with respect to its response to cosmic rays. To characterize the cosmic ray spectra, only multiplicity-2 events were considered. Such events display some interesting features regarding the detectors which get hit in coincidence. Overall, the distribution resembles the overlapping of two effects, which may be related to Compton scattering and cosmic ray events. Due to the specific energy regime and the shape of the scintillators, it was not possible to retrieve a consistent energy distribution. In general, dedicated simulations have

to be run to reproduce the distributions shown in the figures. Such simulations must contain information regarding the shape and relative position of the detectors.

ADDITIONAL ACTIVITIES

For the sake of the activity proposed in the Radioactivity and Nuclear Measurement course, a couple of other activities were run. First, GARFIELD's HV-software was used to bias the CsI preamplifiers one by one. Offset levels were marked down for each preamplifier, both when biased and not biased. Such correlations are necessary to check if the electronics is properly working. Moreover, a test with a ^{60}Co source was performed - analysing the energy spectrum obtained with the scintillators, no full-energy peak was found: the intrinsic resolution is not good enough to get a clear peak.

As far as the analysis is concerned, the arrival time spectra were briefly analysed, finding some meaningful correlation between the time itself and the original chamber. In particular, gating on a certain time interval, most of the data from the backward chamber were cut off. Moreover, the two components of the light signal were analysed - the plot showed a single straight line without any major deviation. Such line, when analysing data from an experiment, is often referred to as the 'neutrals' line.

-
- [1] M. Bruno et al., GARFIELD + RCo digital upgrade: A modern set-up for mass and charge identification of heavy-ion reaction products, Eur. Phys. J. A (2013) 49: 128